INSTITUTE FOR THEORETICAL AND EXPERIMENTAL PHYSICS

FERMILAB-Proposal-0633

A.E.Asratyan, V.I.Efremenko, P.A.Gorichev, V.S.Kaftanov, S.P. Krutchinin, M.A.Kubantsev, I.V.Makhlueva, A.V.Fedotov, V.I.Shekelyan, V.G.Shevchenko -- Institute for Theoretical and Experimental physics, Moscow, USSR ;

V.V.Ammosov, A.G.Denisov, V.A.Gapienko, G.S.Gapienko, V.I.Klukhin, V.I.Koreshev, P.V.Pitukhin, V.I.Sirotenko, E.A.Slobodiuk, V.G. Zaets -- Institute for High Energy Physics, Serpukhov, USSR.

P R O P O S A L

FOR THE STUDY OF NEUTRINO INTERACTIONS IN A BEAM-DUMP EXPERIMENT WITH 15' BUBBLE CHAMBER AT TEVATRON ENERGIES

Moscow 1980

49 pp.

We propose a beam-dump experiment with 15' bubble chamber at the tevatron. The main goal of the experiment is to look for tau-neutrino interactions. Bubble chamber should be filled with heavy neon mixture and placed about 250 meters downstream the high density dump at zero angle. Proton energy should be as high as possible and not less than 800 Gev with total flux of $2.5 * 10^{18}$ p. Tau-neutrinos are produced via F-meson production and subsequent decay. Expected rate of tau-lepton production by ν_τ is ~600 events. These events can be identified by means of a kinematical analysis as well as direct observation of tau-lepton decay vertex at distances of the order of 5 mm from the primary interaction vertex. The latter possibility together with high electron identification efficiency makes the bubble chamber a unique tool for the study of tau-neutrino interactions and tau lifetime. Of equal interest is the possibility to study the high-energy electronic neutrino interactions.

INTRODUCTION

Charged heavy lepton $\tau^{\pm}$ observed in e^+e^- collisions [1] now has the status of a firmly established physical reality. Its sequential origin is the simplest theoretical possibility consistent with the data. It implies the existence of a fundamental lepton doublet formed by τ together with its hypothetical neutral counterpart ν_τ so that the three lepton doublets

$$\begin{pmatrix} \nu_e \\ e^- \end{pmatrix}_L \quad \begin{pmatrix} \nu_\mu \\ \mu^- \end{pmatrix}_L \quad \begin{pmatrix} \nu_\tau \\ \tau^- \end{pmatrix}_L$$

enter the scheme in a completely symmetric way. It equally applies to all couplings of charged currents $(\tilde{\nu}_l l)$ and neutral currents $(\tilde{\nu}_l \nu_l)$ $(l = e, \mu, \tau)$. The observed kinematics of τ decays is consistent with ν_τ being massless.

Obviously this universal scheme can be critically tested only in weak processes involving both $\nu_l \to l$ $(l = \mu, e)$ and $\nu_\tau \to \tau$ transitions (and, possibly, corresponding NC transitions). These fall into two categories :

1. Semileptonic decays of heavy hadrons ($M > m_\tau$) with tau-lepton in the final state ;
2. Tau-lepton production by ν_τ , to be compared with conventional deep-inelastic transitions $\nu_l \to l$ $(l = \mu, e)$.

The existing data based on τ decays are not critical in this respect. In particular, they are insensitive to the overall strength of $(\nu_\tau \tau)$ couplings which a priori might be not equal to G_F after all ($G_\tau \neq G_F$).

None of the tests (1-2) has been performed so far. These tests are not independent since only hadronic decays (1) can serve as a source of ν_τ flux which must be accurately known to perform the comparison (2). However even before the details of "source" heavy particles' production and decay are well understood search for τ production in beam-dump experiments is of great interest since thereby we can hope to :

i) establish the existence of tau-neutrino flux ;
ii) measure τ lifetime and, therefore, G_τ/G_F.

The latter is of fundamental importance and can be carried out exclusively in beam-dump experiments using bubble-chambers in which τ tracks can be directly seen.

Another unique opportunity presented by the combination "beam-dump plus bubble chamber" is the possibility to study high-energy $\nu_e(\tilde{\nu}_e)$ interactions.

This proposal is organised as follows. Section 1 deals with expected prompt and non-prompt neutrino fluxes and event rates. Sections 2 and 3 are devoted to ν_τ and ν_e interactions, respectively. Finally, in Section 4 we discuss some technical aspects of the proposed experiment.

1. NEUTRINO FLUXES AND EVENT RATES

Search for ν_τ interactions in beam-dump experiments was extensively discussed in [2] under the assumption that tau-neutrinos come from the chain decay $F \to \nu_\tau \tau$, $\tau \to \nu_\tau \nu_l l$ of charmed F-mesons produced in proton-nucleus collisions. Charmed D-meson decays account for prompt ν_μ, $\tilde{\nu}_\mu$, ν_e, $\tilde{\nu}_e$ signals rendering them essentially equal.*) The calculated neutrino fluxes (see [3]) are given in Fig. 1 ($2.5*10^{18}$ 1000 protons on copper dump, neutrino detector 250 meters downstream the dump, mass 13 tons, angular acceptance 4 mrad). The latter parameters correspond to 15' bubble chamber filled with heavy neon-hydrogen mixture (64 % neon) with fid. volume of 17 m^3. Expected overall event rates are listed in Table 1.

---

*) We observe that according to the data of preliminary CERN beam-dump run prompt ν_μ and ν_e fluxes could be different [4]. This puzzle must be resolved by the new generation of beam-dump experiments.

2. TAU NEUTRINO INTERACTIONS

2.1. Direct observation of τ tracks. This would enable one to measure τ lifetime and thus give an answer to a crucial question whether or not the couplings of $(\nu_\tau \tau)$ current are governed by universal weak Fermi constant. One might hope to see τ tracks in the bubble chamber since :

i) $|\nu_\tau|$ spectrum is expected to be energetic (see Fig. 1) ;
ii) τ must take a sizable proportion of ν_τ energy ($\sim$.5);
iii) τ is expected to be rather long-lived (lifetime $\sim 3*10^{-13}$ sec for $G_\tau = G_F$).

To probe our chances to actually see τ tracks in the bubble chamber we employed MC simulation of τ neutrino production and decay. Our MC procedure gives an accurate description of τ polarization in leptonic and hadronic decays. Calculations were made in the assumption of $G_\tau = G_F$. Only τ^- production results are displayed for simplicity ; those concerning τ^+ look qualitatively the same and anyway τ^+ production rate is only $\sim$.4 that of τ^- (see Table 1).

Tau decay length distribution (see Fig. 2) is not much help in itself since we need some clear decay signature to identify τ track in a bubble chamber (kink, multiprong, etc). Tau decay modes and branching ratios are listed in Table 2. First we concentrate on kinks. Shown in Fig.3a are angular distributions of decay muons (electrons) from τ^- leptonic decay with a lower cutoff imposed upon τ decay length ($l > .2$, .5, 1. cm). Similar plots dealing with π^- from $\nu_\tau \pi^-$ decay are given in Fig.3b. As evidenced by these plots decay pions yield larger angular deviations from τ momentum direction (and hence more discernible kinks). This is understandable since as it follows from trivial helicity arguments pions are emitted backwards in τ rest frame whereas $\mu^-(e^-)$ are emitted into the forward hemisphere. Plausible criteria that make kink discernible in a bubble chamber are : $l > .5$ cm, $\theta > 2^o$. Then from Fig.3a,b , we conclude that we should observe $\sim$ 4 kinks from each leptonic mode and $\sim$ 4 kinks from pion mode.

Next we make a likely assumption that pion angular distributions of Fig.3b are in fact typical for all hadronic decay modes. Then if we for a moment overlook the possibility of additional decay signatures we can evaluate expected observable kink rates per decay channel. These are listed in the last column of Table 2. Thus under our model assumptions we expect $\sim$30 kinks from τ^- decays (plus $\sim$10 kinks from τ^+ decays).

Other signatures that either facilitate kink analysis or stand in their own right are :

i) for $\nu_\tau \rho^-$ decays with subsequent $\rho^- \to \pi^- \pi^0$, one might hope to identify the π^0 and, finally, reconstruct ρ mass ;

ii) decays involving A_1 or hadron continuum may yield final states with several charged hadrons that yield spectacular signatures (multiprongs or, at least, an abrupt change of ionization).

We conclude that under our model assumptions we expect $\gtrsim$50 events with tau tracks directly visible in the bubble chamber. The backgrounds from charm decays and close-to-vertex interactions seem tracktable. Serious problems could be posed by other tracks overshadowing the tau track.

2.2. Kinematical selection criteria. Kinematical analysis must play an important role in tau signal isolation complementary to the search for direct tau signatures. In case G_τ is significantly larger than G_F this role will obviously be dominant. Hadronic decays (see Table 2) are hard to isolate from conventional NC since the topology is much the same. On the other hand, the topology of tau production with leptonic decay suggests a simple event selection procedure dealing mainly with transverse momenta.

Let $\vec{\pi}$ $(\vec{t}_\ell)$ be the momentum vector of all visible particles in the event (of charged lepton) projected onto the plane transverse to neutrino direction. Typical transverse topologies for both signal and background are shown in Fig. 4 (a,b). Since there are two outgoing neutrinos the tau production event should be significantly disbalanced as compared to normal 1μ for which the unobserved neutral hadrons serve as the only source of transverse disbalance. Furthermore, since in case of tau production the momentum is lost predominantly in the lepton sector, $\vec{\mathcal{T}}$ should tend rather to $\vec{t}_H \equiv \vec{\mathcal{T}} - \vec{t}_\ell$ than $\vec{t}_\ell$. Typical background topology is opposite in this respect since the momentum is lost in the hadron jet (missing neutrals). Therefore we base our treatment on the variables

$$\mathcal{T}_{in} = (\vec{t}_\ell \vec{\mathcal{T}})/|\vec{t}_\ell|, \quad \mathcal{T}_{out} = (\vec{\mathcal{T}}^2 - \mathcal{T}_{in}^2)^{1/2} \qquad (2)$$

(note that by definition T_{in} is not necessarily positive whereas T_{out} is). Given in Fig. 5 are distributions in T_{in} with additional T_{out} cuts . Superimposed are the experimental data of Fermilab-Moscow-Michigan-Serpukhov group ($E_\nu >$ 40 Gev) suitably renormalized. These give some idea of the expected (prompt) background.

If necessary a further cut in either of the variables

$$E_\ell, \quad t_\ell \equiv |\vec{t}_\ell|, \quad x_{vis} \qquad (3)$$

could be employed (see Figs. 6-8). As compared to the background the tau signal is concentrated at small E_ℓ , t_ℓ and x_{vis}. From Fig. 6 we also conclude that expected lepton energy from tau decay is not too high to be accurately measured.

So far as tau hadronic decay modes are concerned (as well as the "authentic" neutral current $\nu_\tau \to \nu_\tau$), the analysis based upon the comparison of E_H plots for NC and CC samples could prove useful. In particular, NC E_H plot should be enhanced towards the highest energies as compared to CC one. This however looks like a job for large electronic detectors (the cut $E_H > 250$ Gev increases the NC/CC ratio by ~ 16 %).

3. INTERACTIONS OF ELECTRON NEUTRINO

3.1. $\nu_\mu - \nu_e$ universality in semileptonic neutral currents. Universality of charged currents $(\nu_\mu \mu^-)$ and $(\nu_e e^-)$ is supported by both hadron decay and preliminary deep-inelastic ν_e scattering data. The manifestation of this universality implicit in the production model 2,3 is the equality of expected ν_μ and ν_e prompt fluxes (see Fig.1 and Table 1).

Contrary to this, the universality of neutral currents $(\tilde{\nu}_\mu \nu_\mu)$ and $(\tilde{\nu}_e \nu_e)$ is still an open question from experimental viewpoint. The almost obvious way to confirm (or disprove) it is to measure the NC/CC ratio for the complete event sample (see Table 1). At this point we observe that the bulk of ν_τ interactions (~70%) lead to final states without charged leptons and hence contribute to NC sample. NC and CC contributions due to tau-neutrino interactions can, however, be subtracted and, anyway, are unlikely to shift the overall NC/CC ratio by more than 3%.

3.2. Diagonal lepton interaction. The diagonal lepton interactic

$$(\tilde{\nu}_e \nu_l)(\tilde{l} l) \qquad (l = \mu, e) \qquad (4)$$

is of fundamental interest since it picks up contributions from both W and Z exchanges (see Fig. 9). Thus it is sensitive to the relative phase between NC and CC leptonic couplings. In the muon sector, its unique manifestation is muon pair production in Coulomb field since there are no muon targets. Instead, there are electron ones, and that constitutes a major advantage of ν_e beam over ν_μ beam. Indeed, the leptonic sector of the diagonal interaction (4) can be explored in the processes

$$\nu_e e^- \to \nu_e e^-, \quad \tilde{\nu}_e e^- \to \tilde{\nu}_e e^- \qquad (5)$$

with pure Z-exchange transitions

$$\nu_\mu e^- \to \nu_\mu e^-, \quad \tilde{\nu}_\mu e^- \to \tilde{\nu}_\mu e^- \qquad (6)$$

as background. The expected rates for (5) and (6) are given in Table 3 within Weinberg-Salam as well as $(V-A)$ assumptions. As reflected in the Table, W.-S. scheme predicts destructive interference between W and Z - exchange amplitudes. Had the interference been constructive, overall (5) plus (6) event rate would be approximately doubled. Thus we have a very nice opportunity to test the validity of W.-S. model.

4. TECHNICAL ASPECTS

In this section we reflect on the broad range of experimental possibilities of the bubble chamber explicitly or implicitly relied on in the above treatment.

1) Instrumental for the beam dump experiment is the ability of the detector to identify both muons and electrons. Two-plane EMI is needed to secure $>95\%$ muon identification efficiency. That for electron detection is $\sim 85\%$ taking into account all possible signatures (brems, tridents, etc.) [5]. The planned internal picket fence (IPF) will increase the efficiency as well as significantly improve the electron momentum measurement accuracy for $p_e > 10$ Gev ($\Delta p/p \approx .3 * p^{-0.5}$). This is of great value for the study of both tau leptonic decays and electron neutrino interactions (see Sections 2-3) which typically yield energetic electrons.

2) For the direct search for tau tracks one obviously needs good space resolution near the event vertex (see Figs. 2-3). That of the 15' bubble chamber with the existing optics is ~ 2 mm. This should be improved considerably when the new optical system is installed.

3) The bubble chamber allows for the detailed study of event topology including v-zeros, gammas, kinks, etc. This is crucial for both tau production event selection procedure (see Section 2) and the proposed study of $\nu_e (\bar{\nu}_e) e^-$ - scattering (Section 3).

4) Finally, we observe that with the bubble chamber we can both reconstruct the incident neutrino energy (with accuracy of $\sim 15\%$) and collect a statistically meaningful sample (see Table 1).

SUMMARY

We conclude that bubble chamber creates an excellent opportunity for two complementary approaches to tau-neutrino signal isolation :

i) search for visible tau tracks and decay signatures ;

ii) kinematical analysis of tau leptonic decays.

The overall magnitude of tau sample is proportional to

$$R \equiv (G_\tau / G_F)^4$$

If $R \gg 1$, kinematics will indicate a significant effect (effect curves of Sect. 2.2 must generally be renormalized by the factor R), whereas there will be no signatures (i). If $R \ll 1$, there will be spectacular signatures, but not much from kinematics.

Insofar as ν_e $(\tilde{\nu}_e)$ interactions are concerned, beam-dump experiment with bubble chamber furnishes two major opportunities :

i) to check the universality of $(\tilde{\nu}_\mu \nu_\mu)$ and $(\tilde{\nu}_e \nu_e)$ weak neutral currents in semileptonic transitions ;

ii) to study diagonal lepton interaction in ν_e $(\tilde{\nu}_e)$ - electron scattering which is sensitive to relative phase between W and Z exchanges and thus provides an important check on the validity of Weinberg-Salam scheme.

REFERENCES

1. F.B.Heile et al. Nucl Phys. B138, 189 (1978).
2. C.H.Albright, R.E.Shrock. Phys. Lett. 84B, 123 (1979); C.H.Albright, R.Shrock, J.Smith. Phys.Rev. D20, 2177 (1979).
3. S.Mori. Fermilab report TM-848 (January 1979).
4. H.Wachsmuth. Preprint CERN-EP/79-115 (October 1979).
5. J.P.Berge et al. Phys. Lett. 81B, 89 (1979).

FIGURE CAPTIONS

Figure 1. Prompt and conventional neutrino fluxes as calculated by S.Mori [3].

Figure 2. Tau lepton decay length distribution (assuming $G_\tau = G_F$).

Figure 3. (a) Decay muons'(electrons') kink angles with a lower cutoff to tau decay length (range $>$ .2, .5, 1. cm).

(b) The same for pions from tau $\nu_\tau \pi^-$ decay.

Figure 4. (a) Typical transverse topology for tau production with leptonic decay (see text for details).

(b) Same as (a) but for the background.

Figure 5. T_{in} distributions with additional T_{out} cuts ($T_{out} >$ 0, .4, .8 Gev). Given in the same figure are the experimental data of Fermilab-Moscow-Michigan-Serpukhov group ($E_\nu > 40$ Gev) properly renormalized.

Figure 6. Decay (prompt background) lepton momentum distribution.

Figure 7. Decay (prompt background) lepton transverse momentum distribution.

Figure 8. x_{vis} distribution for tau leptonic decay and prompt background events.

Figure 9. W and Z - exchange contributions to diagonal lepton interaction responsible for $\nu_e(\bar{\nu}_e)e^-$ - scattering.

Table 1

Calculated event rates for the proposed beam-dump run

	μ^-	e^-	μ^+	e^+	τ^-	τ^+	NC	Σ
Prompt	16 000	16 000	6 000	6 000	440	180	14 000	58 600
Conventional	6 500	400	1 000	100			2 500	10 500
Σ	22 500	16 400	7 000	6 100	440	180	16 500	68 100

Table 2

Tau lepton decay modes and expected kink rates

decay mode	branching	kinks
$\nu_\tau e^- \tilde{\nu}_e$	.20	4
$\nu_\tau \mu^- \tilde{\nu}_\mu$	.20	4
$\nu_\tau \pi^-$	.11	4
$\nu_\tau \rho^-$	.22	8
$\nu_\tau A_1^-$	.07	2
ν_τ(continuum)	.18	7

Table 3

Calculated rates for neutrino-electron scattering

	ν_μ	$\tilde{\nu}_\mu$	ν_e	$\tilde{\nu}_e$	Σ
W. - S.	2	2	12	5	21
(V-A)	0	0	19	6	25

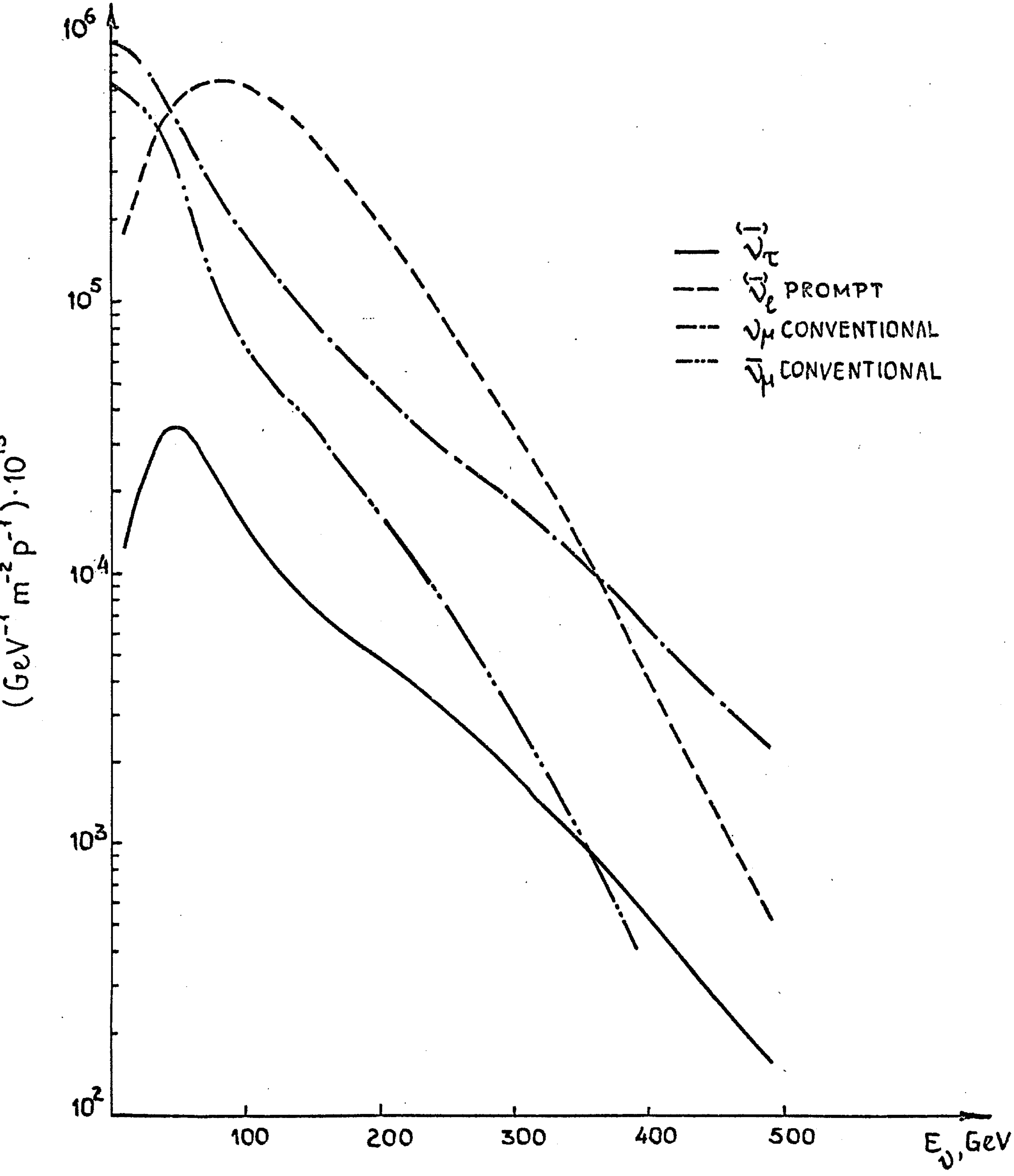
10^6
10^5
10^4
10^3
10^2
$(GeV^{-1} m^{-2} p^{-1}) \cdot 10^{13}$
100
200
300
400
500
E_ν, GeV
$\overset{(-)}{\nu}_\tau$
$\overset{(-)}{\nu}_\ell$ PROMPT
ν_μ CONVENTIONAL
$\bar{\nu}_\mu$ CONVENTIONAL

Fig. 1

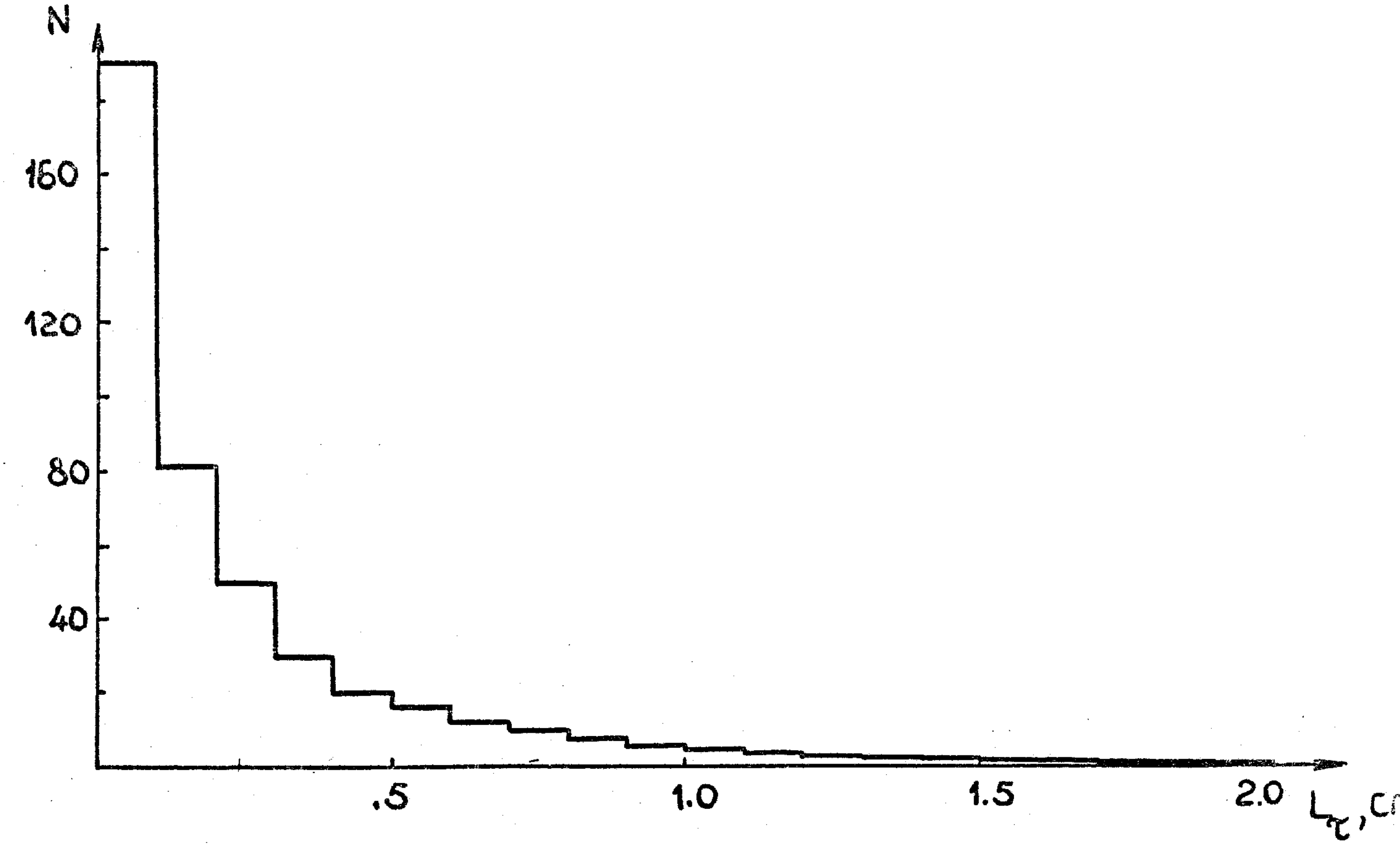

Fig. 2

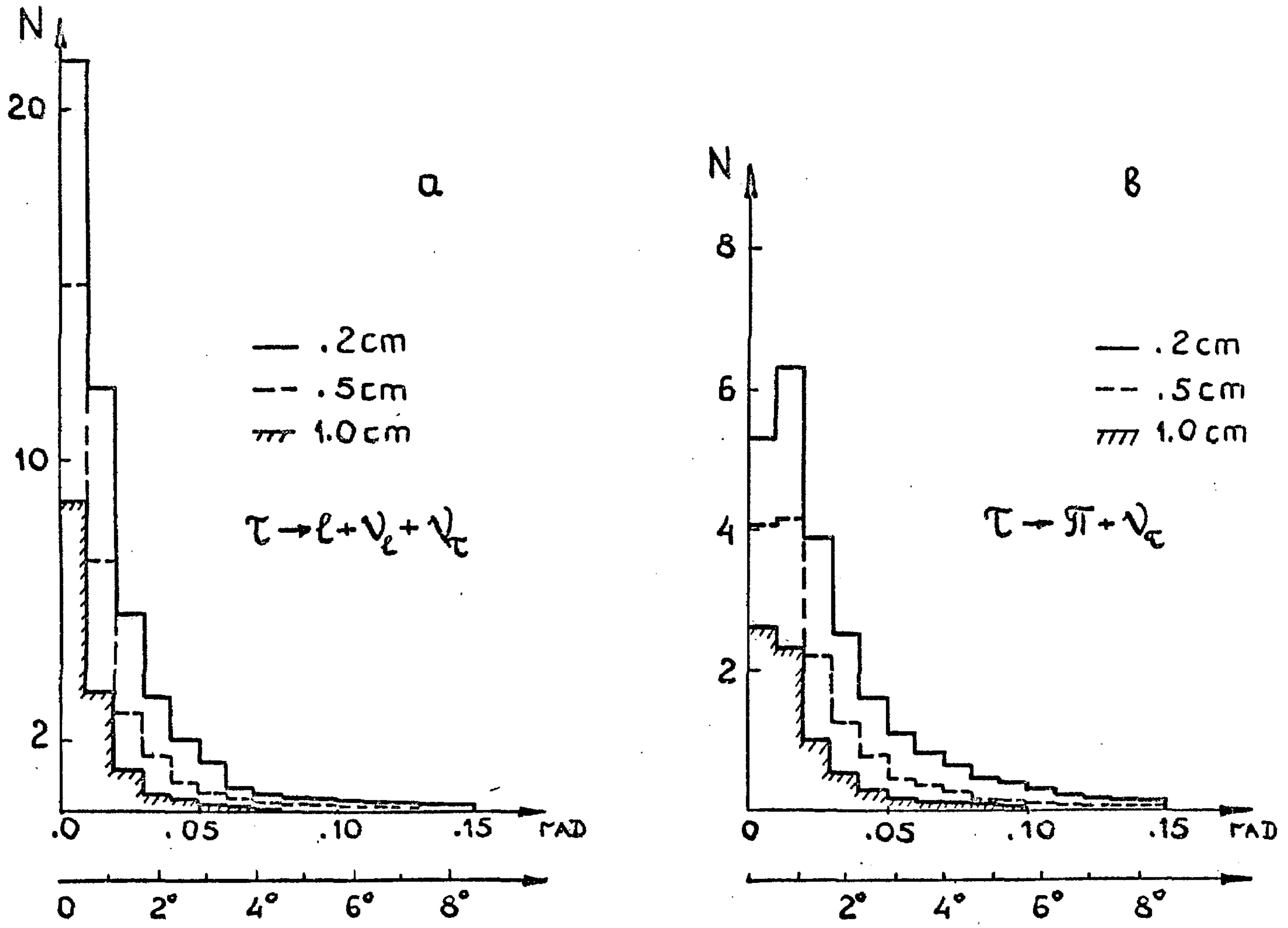
N
20
10
2
a
— .2cm
-- .5cm
1.0cm
τ → ℓ + ν_ℓ + ν_τ
.0
.05
.10
.15
rad
0
2°
4°
6°
8°
N
8
6
4
2
β
— .2cm
-- .5cm
1.0cm
τ → π + ν_τ
0
.05
.10
.15
rad
2°
4°
6°
8°

Fig.3

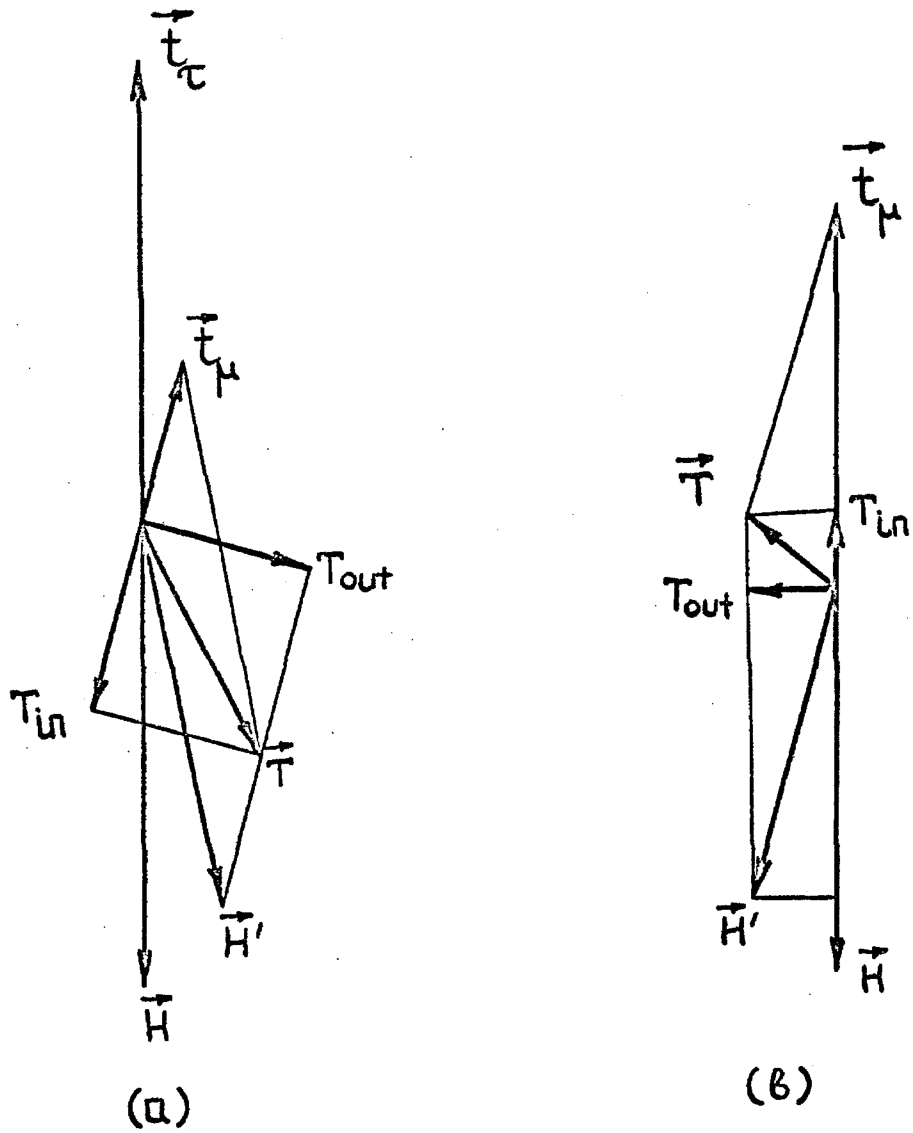

$\vec{t}_\tau$
$\vec{t}_\mu$
T_{out}
T_{in}
$\vec{T}$
$\vec{H}'$
$\vec{H}$
(a)
$\vec{t}_\mu$
$\vec{T}$
T_{in}
T_{out}
$\vec{H}'$
$\vec{H}$
(b)

Fig. 4

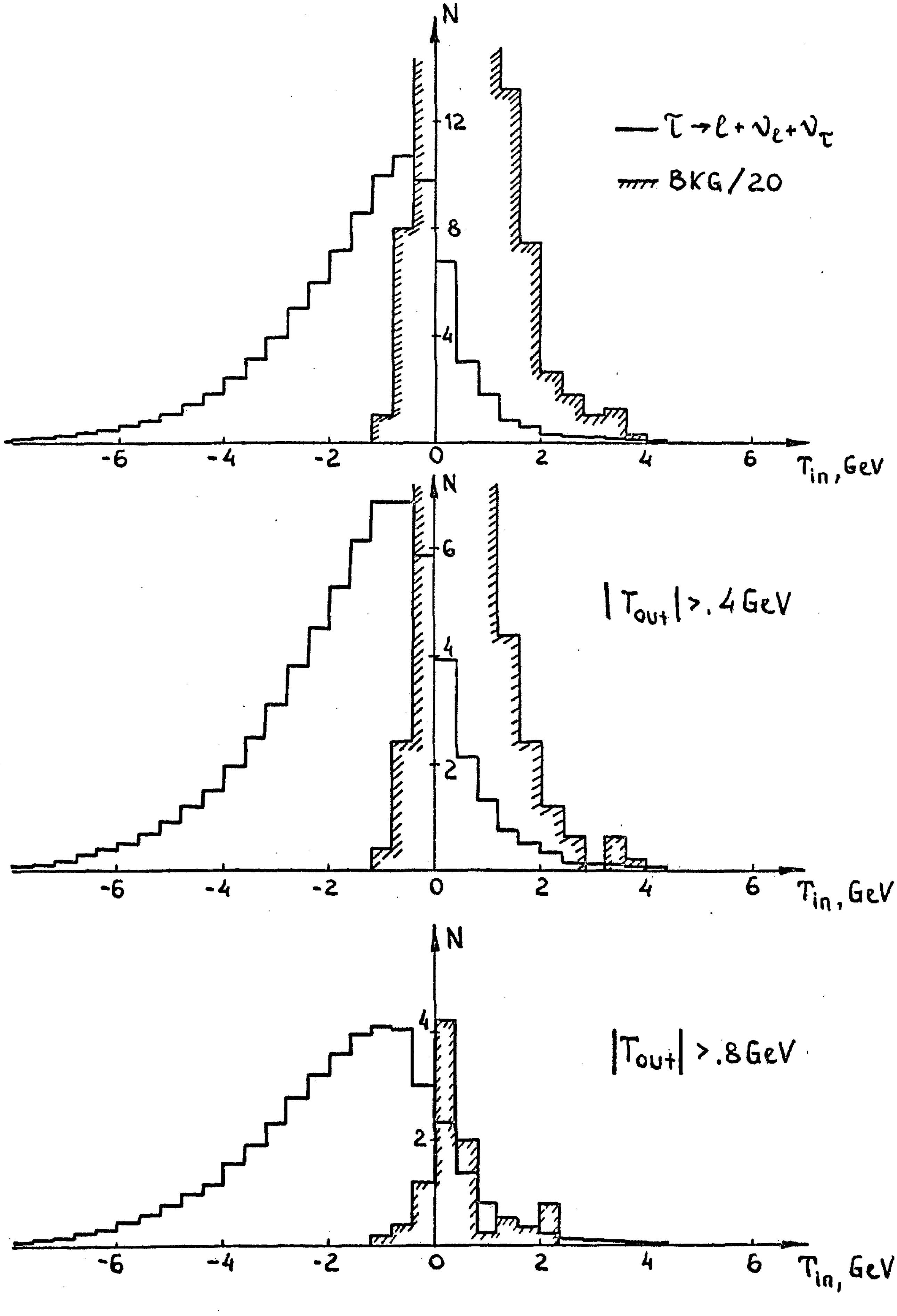

N
12
8
4
$\tau \to \ell + \nu_\ell + \nu_\tau$
BKG/20
-6
-4
-2
0
2
4
6
T_{in}, GeV
N
6
4
2
$|T_{out}| > .4$ GeV
-6
-4
-2
0
2
4
6
T_{in}, GeV
N
4
2
$|T_{out}| > .8$ GeV
-6
-4
-2
0
2
4
6
T_{in}, GeV

Fig.5

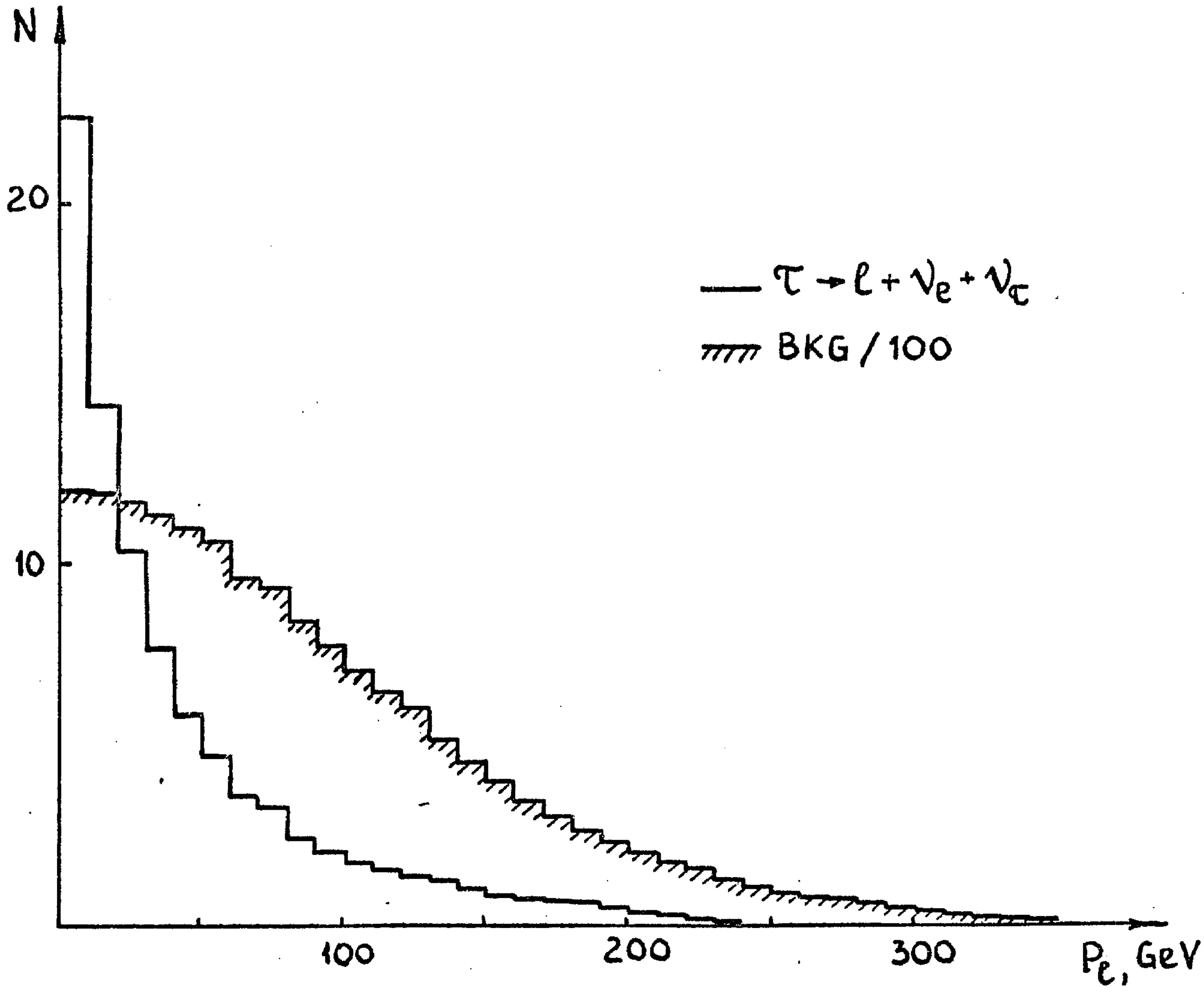

Fig. 6

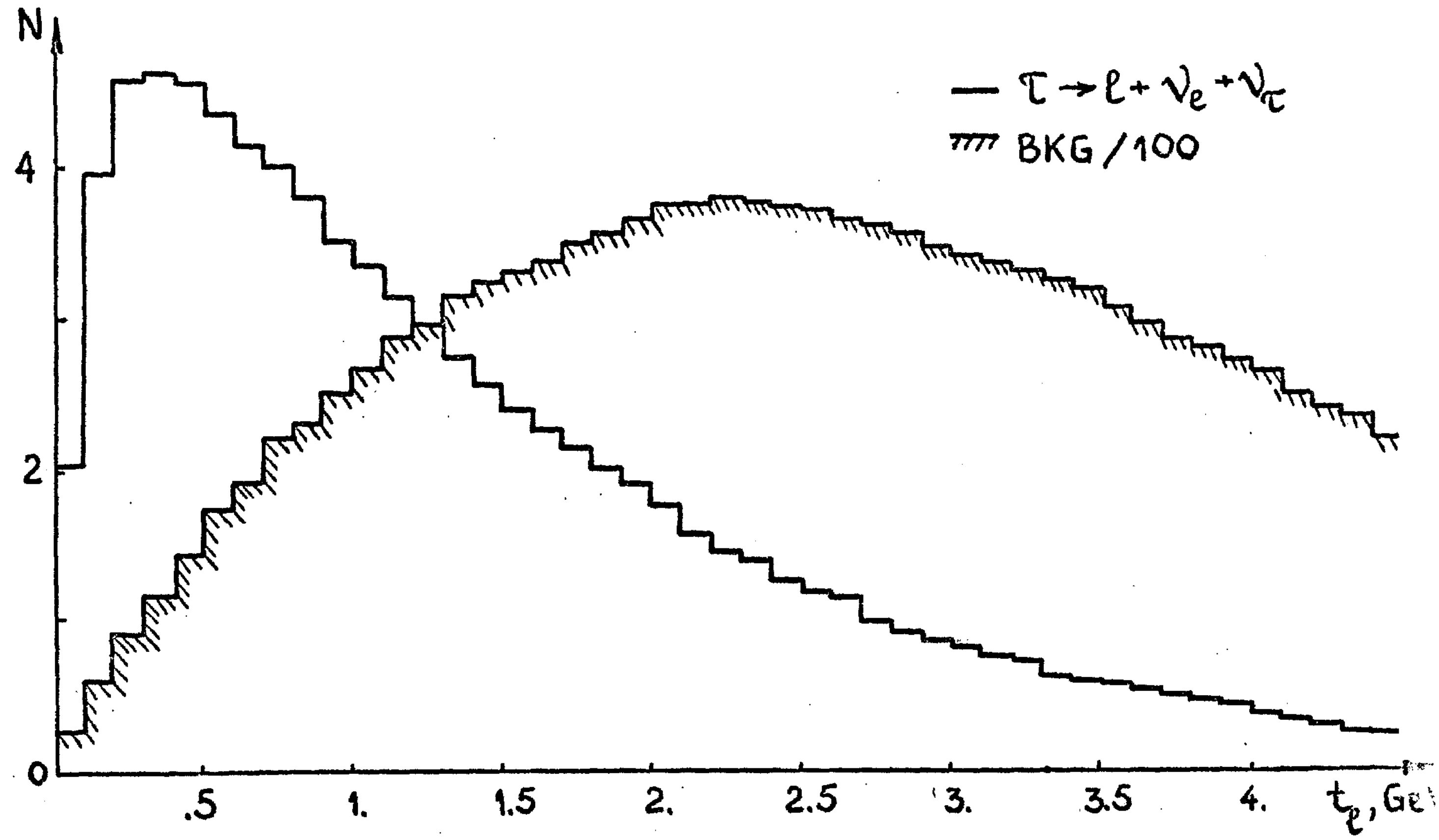

Fig. 7

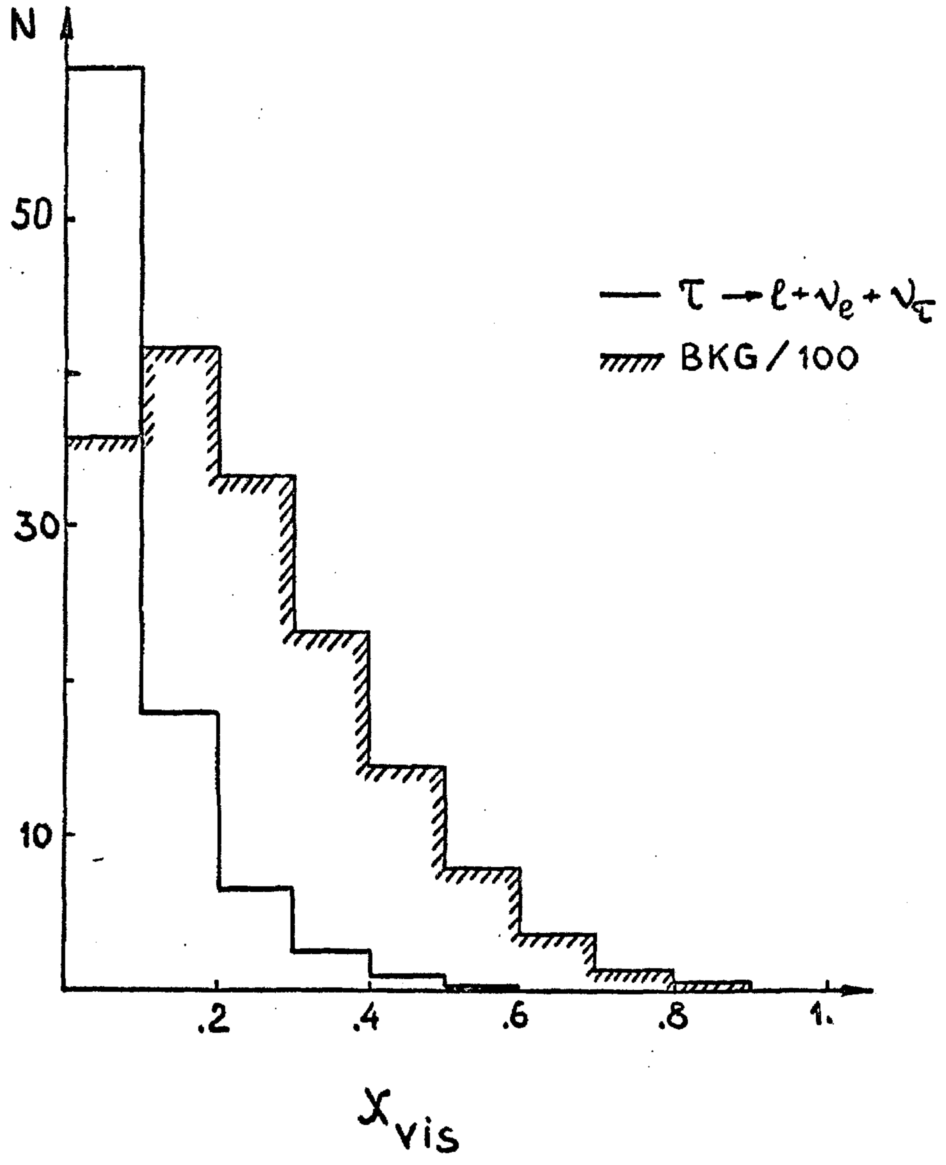

Fig. 8

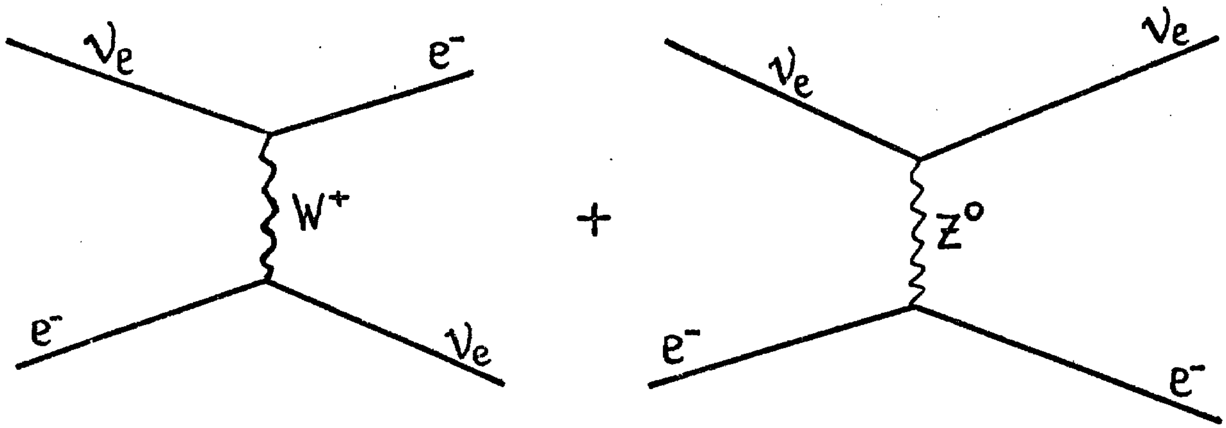

Fig. 9

FERMILAB

Fermilab Proposal 632

Scientific Spokesmen:

V.S. Kaftanov

Institute of Theoretical

and Experimental Physics

Moscow, USSR

V.V. Ammosov

Institute of High Energy

Physics

Serpukhov, USSR

PROPOSAL TO STUDY NEUTRINO INTERACTIONS IN A BEAM-DUMP EXPERIMENT WITH THE 15-FT BUBBLE CHAMBER AT TEVATRON ENERGIES

A.E. Asratyan, V.I. Efremenko, A.V. Fedotov, P.A. Gorichev,
V.S. Kaftanov, S.P. Krutchinin, M.A. Kubantsev, I.V. Makhlueva,
V.I. Shekelyan, V.G. Shevchenko

Institute of Theoretical and Experimental Physics

Moscow, USSR

and

V.V. Ammosov, A.G. Denisov, V.A. Gapienko, G.S. Gapienko,
V.I. Klukhin, V.I. Koreshev, P.V. Pitukhin, V.I. Sirotenko,
E.A. Slobodiuk, V.G. Zaets

Institute of High Energy Physics,

Serpukhov, USSR

April 1980

Abstract

We propose a beam-dump experiment with the 15 ft. bubble chamber at the Tevatron. The main goal of the experiment is to look for ν_τ-interactions. The bubble chamber should be filled with a heavy neon-hydrogen mixture and placed about 250 meters downstream the high density dump at zero angle. Proton energy should be as high as possible and not less than 800 GeV with the total flux of $2.5 * 10^{18}$ protons. τ -neutrinos are produced via F-meson production and a subsequent decay. Expected rate of τ -lepton production by the ν_τ is ~ 600 events. These events can be identified by means of a kinematical analysis as well as by direct observation of the τ -lepton decay vertex at distances of the order of 5mm from the primary interaction vertex. The latter possibility together with high electron identification efficiency makes the bubble chamber a unique tool for the study of τ -neutrino interactions and τ-lepton lifetime.

Of equal interest is the possibility to study the high energy interactions where the following two major topics are considered:

1) the universality of the $(\nu_\mu \nu_\mu)$ and $(\nu_e \nu_e)$ weak neutral currents in semileptonic transitions;
2) diagonal interactions in the $\nu_e(\bar{\nu}_e)$ - electron scattering which reflects the relative phase between the W and Z^o exchanges and provides an important check of the Weinberg-Salam model.

INTRODUCTION

Charged heavy lepton $\tau^{\pm}$ observed in e^+e^- collisions [1] now has the status of a firmly established physical reality. Its sequential origin is the simplest theoretical possibility consistent with the data. It implies the existence of a fundamental lepton doublet formed by τ together with its hypothetical neutral counterpart ν_τ so that the three lepton doublets

$$\begin{pmatrix} \nu_e \\ e^- \end{pmatrix}_L \quad \begin{pmatrix} \nu_\mu \\ \mu^- \end{pmatrix}_L \quad \begin{pmatrix} \nu_\tau \\ \tau^- \end{pmatrix}_L$$

enter the scheme in a completely symmetric way. It equally applies to all couplings of charged currents $(\tilde{\nu}_\ell \ell)$ and neutral currents $(\tilde{\nu}_\ell \nu_\ell)$ $(\ell = e, \mu, \tau)$. The observed kinematics of τ decays is consistent with ν_τ being massless.

Obviously this universal scheme can be critically tested only in weak processes involving both $\nu_\ell \to \ell$ $(\ell = \mu, e)$ and $\nu_\tau \to \tau$ transitions (and, possibly, corresponding NC transitions). These fall into two categories:

1. Semileptonic decays of heavy hadrons $(M > m_\tau)$ with tau-lepton in the final state;
2. Tau-lepton production by ν_τ, to be compared with conventional deep-inelastic transitions $\nu_\ell \to \ell$ $(\ell = \mu, e)$.

The existing data based on τ decays are not critical in this respect. In particular, they are insensitive to the overall strength of $(\nu_\tau \tau)$ couplings which a priori might be not equal to G_F after all $(G_\tau \neq G_F)$.

None of the tests (1-2) has been performed so far. These tests are not independent since only hadronic decays (1) can serve as a source of ν_τ flux which must be accurately known to perform the comparison (2). However even before the details of "source" heavy particles' production and decay are well understood search for τ production in beam-dump experiments is of great interest since thereby we can hope to:

i) establish the existence of tau-neutrino flux;

ii) measure τ lifetime and, therefore, G_τ/G_F.

The latter is of fundamental importance and can be carried out exclusively in beam-dump experiments using bubble chambers in which τ tracks can be directly seen.

Another unique opportunity presented by the combination "beam-dump plus bubble chamber" is the possibility to study high-energy $\nu_e(\tilde{\nu}_e)$ interactions.

This proposal is organised as follows. Section 1 deals with expected prompt and non-prompt neutrino fluxes and event rates. Sections 2 and 3 are devoted to ν_τ and ν_e interactions, respectively. Finally, in Section 4 we discuss some technical aspects of the proposed experiment.

1. NEUTRINO FLUXES AND EVENT RATES

Search for ν_τ interactions in beam-dump experiments was extensively discussed in [2] under the assumption that tau-neutrinos come from the chain decay $F \to \nu_\tau \tau$, $\tau \to \nu_\tau \nu_\ell \ell$ of charmed F-mesons produced in proton-nucleus collisions. Charmed D-meson decays account for prompt ν_μ, $\tilde{\nu}_\mu$, ν_e, $\tilde{\nu}_e$ signals rendering them essentially equal.*) The calculated neutrino fluxes (see [3]) are given in Fig. 1 ($2.5*10^{18}$ protons with energy 1000 GeV on copper dump, a neutrino detector 250 meters downstream the dump, mass 13 tons, angular acceptance 4 mrad). The latter parameters correspond to 15 ft. bubble chamber filled with heavy neon-hydrogen mixture (64% neon) with fid. volume of 17 m^3. Expected overall event rates are listed in Table 1.

---

*) We observe that according to the data of preliminary CERN beam-dump run prompt ν_μ and ν_e fluxes could be different [4]. This puzzle must be resolved by the new generation of beam-dump experiments.

2. TAU NEUTRINO INTERACTIONS

<u>2.1. Direct observation of τ tracks.</u> This would enable one to measure τ lifetime and thus give an answer to a crucial question whether or not the couplings of $(\nu_\tau \tau)$ current are governed by universal weak Fermi constant. One might hope to see τ tracks in the bubble chamber since:

i) ν_τ spectrum is expected to be energetic (see Fig. 1);

ii) τ must take a sizable proportion of ν_τ energy ($\sim$.5);

iii) τ is expected to be rather long-lived (lifetime $\sim 3*10^{-13}$ sec for $G_\tau = G_F$).

To probe our chances to actually see τ tracks in the bubble chamber we employed MC simulation of τ neutrino production and decay. Our MC procedure gives an accurate description of τ polarization in leptonic and hadronic decays. Calculations were made in the assumption of $G_\tau = G_F$. Only τ^- production results are displayed for simplicity; those concerning τ^+ look qualitatively the same and anyway τ^+ production rate is only $\sim .4$ that of τ^- (see Table 1).

Tau decay length distribution (see Fig. 2) is not much help in itself since we need some clear decay signature to identify τ track in a bubble chamber (kink, multiprong, etc). Tau decay modes and branching ratios are listed in Table 2. First we concentrate on kinks. Shown in Fig. 3a are angular distributions of decay muons (electrons) from τ leptonic decay with a lower cutoff imposed upon τ decay length ($r > .2, .5, .1$ cm). Similar plots dealing with π^- from $\nu_\tau \pi^-$ decay are given in Fig. 3b. As evidenced by these plots decay pions yield larger angular deviations from τ momentum direction (and hence more discernible kinks). This is understandable since as it follows from trivial helicity arguments pions are emitted backwards in τ rest frame whereas $\mu^-(e^-)$ are emitted into the forward hemisphere. Plausible criteria that make kink discernible in a bubble chamber are: $r > .5$ cm, $\theta > 2^o$. Then from Fig. 3a,b we conclude that we should observe ~ 4 kinks from each leptonic mode and ~ 4 kinks from pion mode.

Next we make a likely assumption that pion angular distributions of Fig. 3b are in fact typical for all hadronic decay modes. Then if we for a moment overlook the possibility of additional decay signatures we can evaluate expected observable kink rates per decay channel. These are listed in the last column of Table 2. Thus under our model assumptions we expect ~ 30 kinks from τ^- decays (plus ~ 10 kinks from τ^+ decays).

Other signatures that either facilitate kink analysis or stand in their own right are:

i) for $\nu_\tau\rho^-$ decays with subsequent $\rho^- \rightarrow \pi^-\pi^o$, one might hope to identify the π^o and, finally, reconstruct ρ mass;

ii) decays involving A_1 or hadron continuum may yield final states with several charged hadrons that yield spectacular signatures (multiprongs or, at least, an abrupt change of ionization).

We conclude that under our model assumptions we expect $\gtrsim$ 50 events with tau tracks directly visible in the bubble chamber. The backgrounds from charm decays and close-to-vertex interactions seem tracktable. Serious problems could be posed by other tracks overshadowing the tau track.

2.2 Kinematical selection criteria. Kinematical analysis must play an important role in tau signal isolation complementary to the search for direct tau signatures. In case G_τ is significantly larger than G_F this role will obviously be dominant. Hadronic decays (see Table 2) are hard to isolate from conventional NC since the topology is much the same. On the other hand, the topology of tau production with leptonic decay suggests a simple event selection procedure dealing mainly with transverse momenta.

Let $\vec{T}$ ($\vec{t}_\ell$) be the momentum vector of all visible particles in the event (of charged lepton) projected onto the plane transverse to the neutrino direction. Typical transverse topologies for both signal and background are shown in Fig. 4(a,b). Since there are two outgoing neutrinos the tau production event should be significantly disbalanced as compared to normal 1μ for which the unobserved neutral hadrons serve as the only source of transverse disbalance. Furthermore, since in case of tau production the momentum is lost predominantly in the lepton sector, $\vec{T}$ should tend rather to $\vec{t}_H \equiv \vec{T} - \vec{t}_\ell$ than $\vec{t}_\ell$. Typical background topology is opposite in this respect since the momentum is lost in the hadron jet (missing neutrals). Therefore we base our treatment on the variables

$$T_{in} = (\vec{t}_\ell \vec{T})/|\vec{t}_\ell| , \quad T_{out} = (\vec{T}^2 - T_{in}^2)^{1/2} \qquad (2)$$

(note that by definition T_{in} is not necessarily positive whereas T_{out} is). Given in Fig. 5 are distributions in T_{in} with additional T_{out} cuts. Superimposed are the experimental data of Fermilab-Moscow-Michigan-Serpukhov group ($E_\nu > 40$ GeV) suitably renormalized. These give some idea of the expected (prompt) background.

If necessary a further cut in either of the variables

$$E_\ell , \; t_\ell \equiv |\vec{t}_\ell| , \; x_{vis} \qquad (3)$$

could be employed (see Figs. 6-8). As compared to the background the tau signal is concentrated at small E_ℓ, t_ℓ and x_{vis}. From Fig. 6 we also conclude that expected lepton energy from tau decay is not too high to be accurately measured.

So far as tau hadronic decay modes are concerned (as well as the "authentic" neutral current $\nu_\tau \to \nu_\tau$), the analysis based upon the comparison of E_H plots for NC and CC samples could prove useful. In particular, NC E_H plot should be enhanced towards the highest energies as compared to CC one. This however looks like a job for large electronic detectors (the cut $E_H > 250$ GeV increases the NC/CC ratio by ~ 16%).

3. INTERACTIONS OF ELECTRON NEUTRINO

3.1 $\nu_\mu - \nu_e$ universality in semileptonic neutral currents.

Universality of charged currents $(\nu_\mu \mu^-)$ and $(\nu_e e^-)$ is supported by both hadron decay and preliminary deep-inelastic ν_e scattering data. The manifestation of this universality implicit in the production model [2,3] is the equality of expected ν_μ and ν_e prompt fluxes (see Fig. 1 and Table 1).

Contrary to this, the universality of neutral currents $(\tilde{\nu}_\mu \nu_\mu)$ and $(\tilde{\nu}_e \nu_e)$ is still an open question from experimental viewpoint. The almost obvious way to confirm (or disprove) it is to measure the NC/CC ratio for the complete event sample (see Table 1). At this point we observe that the bulk of ν_τ interactions (~70%) lead to final states without charged leptons and hence contribute to NC sample. NC and CC contributions due to tau-neutrino interactions can, however, be subtracted and, anyway, are unlikely to shift the overall NC/CC ratio by more than 3%.

3.2 Diagonal lepton interaction.

The diagonal lepton interaction

$$(\tilde{\nu}_\ell \nu_\ell)\ (\tilde{\ell}\ell) \qquad (\ell = \mu, e) \tag{4}$$

is of fundamental interest since it picks up contributions from both W and Z exchanges (see Fig. 9). Thus it is sensitive to the relative phase between NC and CC leptonic couplings.

In the muon sector, its unique manifestation is muon pair production in Coulomb field since there are no muon targets. Instead, there are electron ones, and that constitutes a major advantage of ν_e beam over ν_μ beam. Indeed, the leptonic sector of the diagonal interaction (4) can be explored in the processes

$$\nu_e e^- \to \nu_e e^-, \; \tilde{\nu}_e e^- \to \tilde{\nu}_e e^- \tag{5}$$

with pure Z-exchange transitions

$$\nu_\mu e^- \to \nu_\mu e^-, \; \tilde{\nu}_\mu e^- \to \tilde{\nu}_\mu e^- \tag{6}$$

as background. The expected rates for (5) and (6) are given in Table 3 within Weinberg-Salam (W.-S.) as well as (V-A) assumptions. As reflected in the Table, W.-S. scheme predicts destructive interference between W and Z - exchange amplitudes. Had the interference been constructive, overall (5) plus (6) event rate would be approximately doubled. Thus we have a very nice opportunity to test the validity of W.-S. model.

4. TECHNICAL ASPECTS

In this section we reflect on the broad range of experimental possibilities of the bubble chamber explicitly or implicitly relied on in the above treatment.

1) Instrumental for the beam dump experiment is the ability of the detector to identify both muons and electrons. Two-plane EMI is needed to secure > 95% muon identification efficiency. That for electron detection is ~ 85% taking into account all possible signatures (brems, tridents, etc.) [5]. The planned internal shower picket fence [6] (ISPF) will increase the efficiency as well as significantly improve the electron momentum measurement accuracy for p_e >10 GeV ($\Delta p/p \approx .3*p^{-0.5}$). This is of great value for the study of both tau leptonic decays and electron neutrino interactions (see Section 2-3) which typically yield energetic electrons.

2) For the direct search for tau tracks one obviously needs good space resolution near the event vertex (see Figs. 2-3). That of the 15 ft. bubble chamber with the existing optics is ~ 2 mm. This should be improved considerably when the new optical system is installed.

3) The bubble chamber allows for the detailed study of event topology including V-zeros, gammas, kinks, etc. This is crucial for both tau production event selection procedure (see Section 2) and the proposed study of $\nu_e(\bar{\nu}_e)$ e^- - scattering (Section 3).

4) Finally, we observe that with the bubble chamber we can both reconstruct the incident neutrino energy (with accuracy of ~15%) and collect a statistically meaningful sample (see Table 1).

SUMMARY

We conclude that bubble chamber creates an excellent opportunity for two complementary approaches to tau-neutrino signal isolation:

i) search for visible tau tracks and decay signatures;

ii) kinematical analysis of tau leptonic decays.

The overall magnitude of the tau sample is proportional to

$$R \equiv (G_\tau/G_F)^4$$

If R>>1, kinematics will indicate a significant effect (effect curves of Sect. 2.2 must generally be renormalized by the factor R), whereas there will be no signatures (i). If R<<1, there will be spectacular signatures, but not much from kinematics.

Insofar as $\nu_e(\tilde{\nu}_e)$ interactions are concerned, beam-dump experiment with the bubble chamber furnishes two major opportunities:

i) to check the universality of $(\tilde{\nu}_\mu\nu_\mu)$ and $(\tilde{\nu}_e\nu_e)$ weak neutral currents in semileptonic transitions;

ii) to study diagonal lepton interaction in $\nu_e(\tilde{\nu}_e)$ - electron scattering which is sensitive to relative phase between W and Z exchanges and thus provides an important check on the validity of Weinberg-Salam scheme.

REFERENCES

1. F.B. Heile et al. Nucl. Phys. B138, 189(1978).

2. C.H. Albright, R.E. Shrock, Phys. Lett. 84B, 123(1979); C.H. Albright, R. Shrock, J. Smith, Phys. Rev. D20, 2177(1979).

3. S. Mori, Fermilab report TM-848 (January 1979).

4. H. Wachsmuth, Preprint CERN-EP/79-115 (October 1979).

5. J.P. Berge et al., Phys. Lett. 81B, 89(1979).

6. V.V. Ammosov et al., Proposal to Study Neutrino and Antineutrino Interactions in Deuterium with 15 ft. bubble chamber at Tevatron Energies, April 1980.

FIGURE CAPTIONS

Figure 1: Prompt and conventional neutrino fluxes as calculated by S. Mori [3].

Figure 2: Tau lepton decay length distribution (assuming $G_\tau = G_F$).

Figure 3: (a) Decay muons' (electrons') kink angles with a lower cutoff to tau decay length (range > .2, .5, 1. cm).

(b) The same for pions from tau $\nu_\tau \pi^-$ decay.

Figure 4: (a) Typical transverse topology for tau production with leptonic decay (see text for details).

(b) Same as (a) but for the background.

Figure 5: T_{in} distributions with additional T_{out} cuts ($T_{out} > 0$, .4, .8 GeV). Given in the same figure are the experimental data of Fermilab-Moscow-Michigan-Serpukhov group ($E_\nu > 40$ GeV) properly renormalized.

Figure 6: Decay (prompt background) lepton momentum distribution.

Figure 7: Decay (prompt background) lepton transverse momentum distribution.

Figure 8: x_{vis} distribution for tau leptonic decay and prompt background events.

Figure 9: W and Z - exchange contributions to diagonal lepton interaction responsible for $\nu_e(\bar{\nu}_e)e^-$ - scattering.

Table 1

Calculated event rates for the proposed beam-dump run

	μ^-	e^-	μ^+	e^+	τ^-	τ^+	NC	Σ
Prompt	16 000	16 000	6 000	6 000	440	180	14 000	58 600
Conventional	6 500	400	1 000	100			2 500	10 500
Σ	22 500	16 400	7 000	6 100	440	180	16 500	68 100

Table 2

Tau lepton decay modes and expected kink rates

decay mode	branching	kinks
$\nu_\tau e^- \tilde{\nu}_e$	.20	4
$\nu_\tau \mu^- \tilde{\nu}_\mu$	.20	4
$\nu_\tau \pi^-$	.11	4
$\nu^\tau \rho^-$	.22	8
$\nu_\tau A_1^-$	.07	2
ν_τ (continuum)	.18	7

Table 3

Calculated rates for neutrino-electron scattering

	ν_μ	$\tilde{\nu}_\mu$	ν_e	$\tilde{\nu}_e$	Σ
W. - S.	2	2	12	5	21
(V-A)	0	0	19	6	25

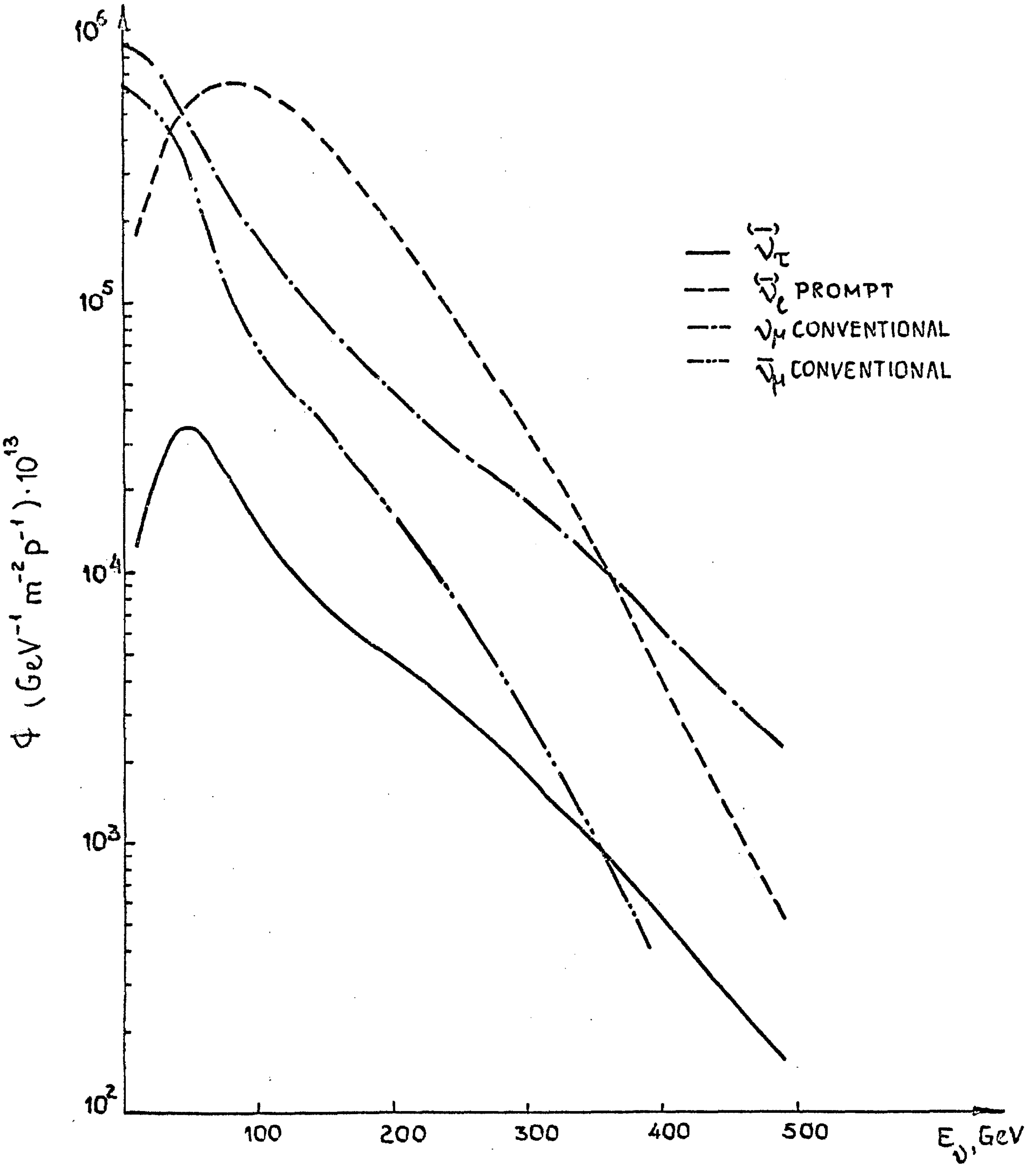
10^6
10^5
10^4
10^3
10^2
Φ $(GeV^{-1} m^{-2} p^{-1}) \cdot 10^{13}$
100
200
300
400
500
E_ν, GeV
$\overset{(-)}{\nu}_\tau$
$\overset{(-)}{\nu}_\ell$ PROMPT
ν_μ CONVENTIONAL
$\bar{\nu}_\mu$ CONVENTIONAL

Fig. 1

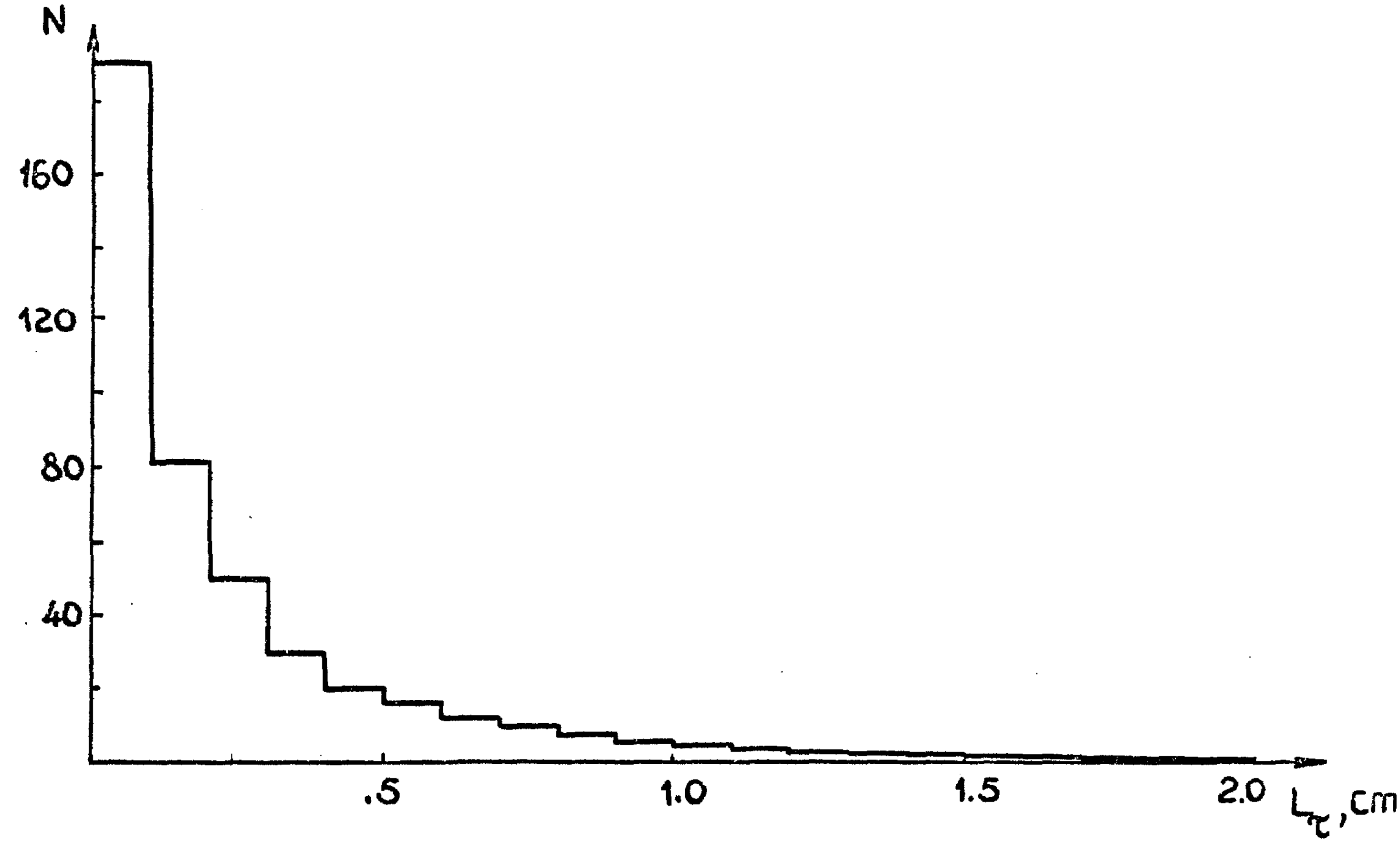

Fig.2

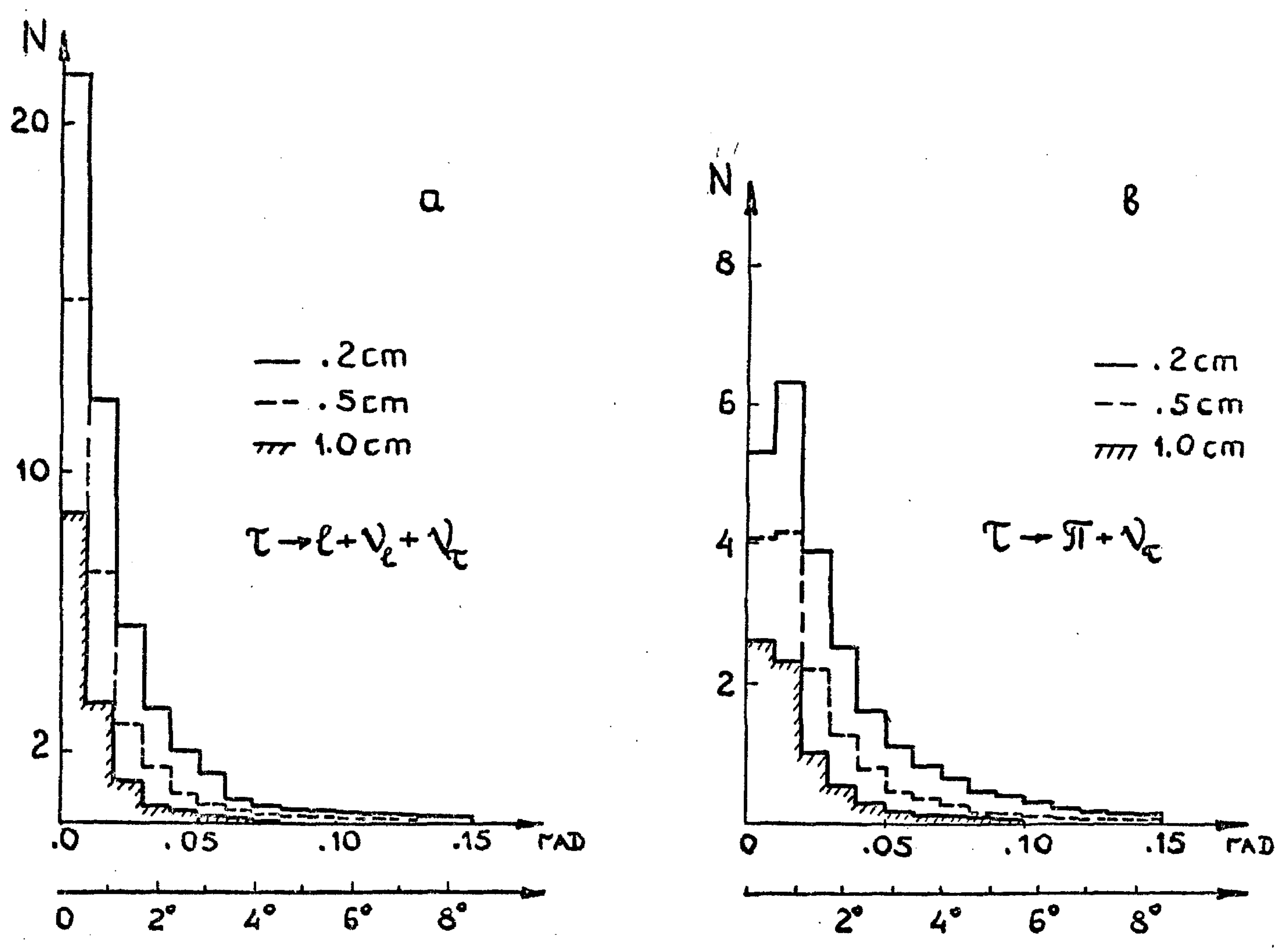
N
20
10
2
a
.2cm
.5cm
1.0cm
τ→ℓ+ν_ℓ+ν_τ
.0
.05
.10
.15
rAD
0
2°
4°
6°
8°
N
8
6
4
2
b
.2cm
.5cm
1.0cm
τ→π+ν_τ
0
.05
.10
.15
rAD
2°
4°
6°
8°

Fig.3

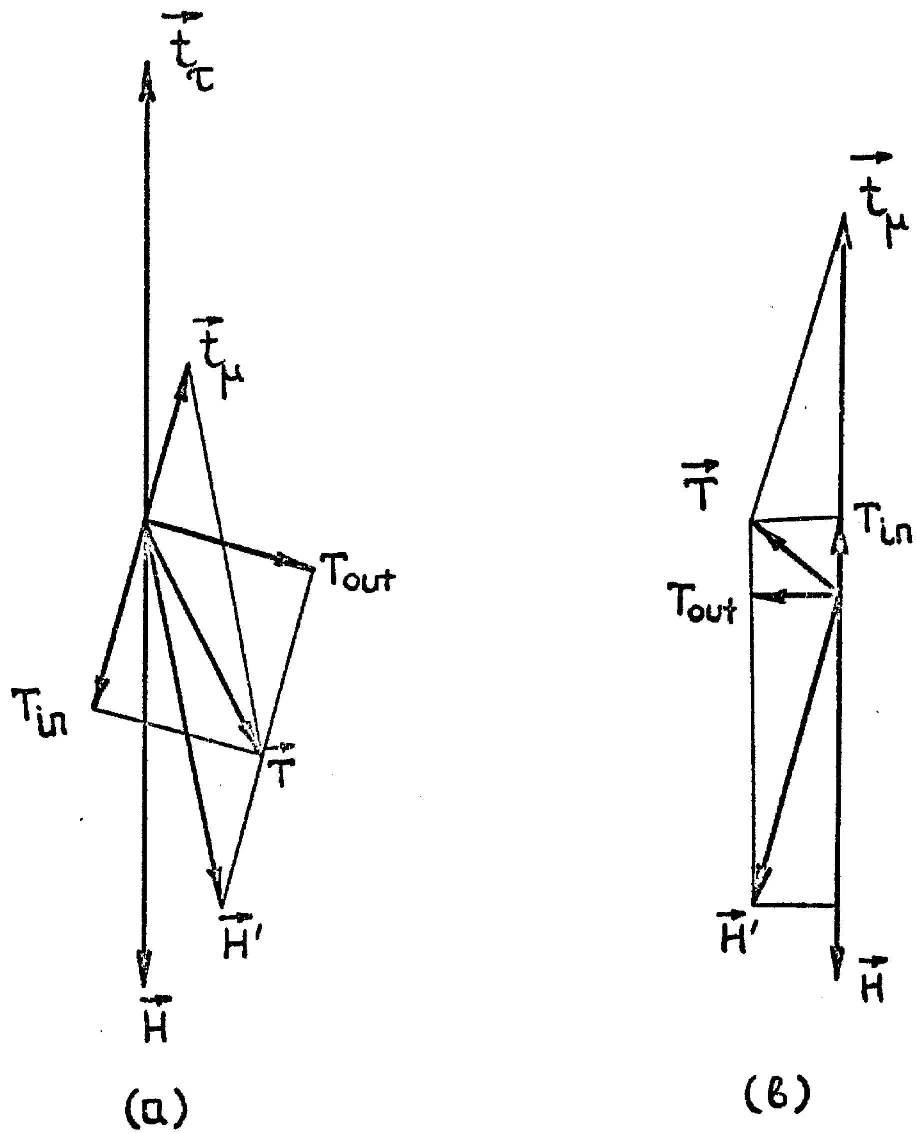

$\vec{t}_\tau$
$\vec{t}_\mu$
T_{out}
T_{in}
$\vec{T}$
$\vec{H}'$
$\vec{H}$
(a)
$\vec{t}_\mu$
$\vec{T}$
T_{in}
T_{out}
$\vec{H}'$
$\vec{H}$
(b)

Fig. 4

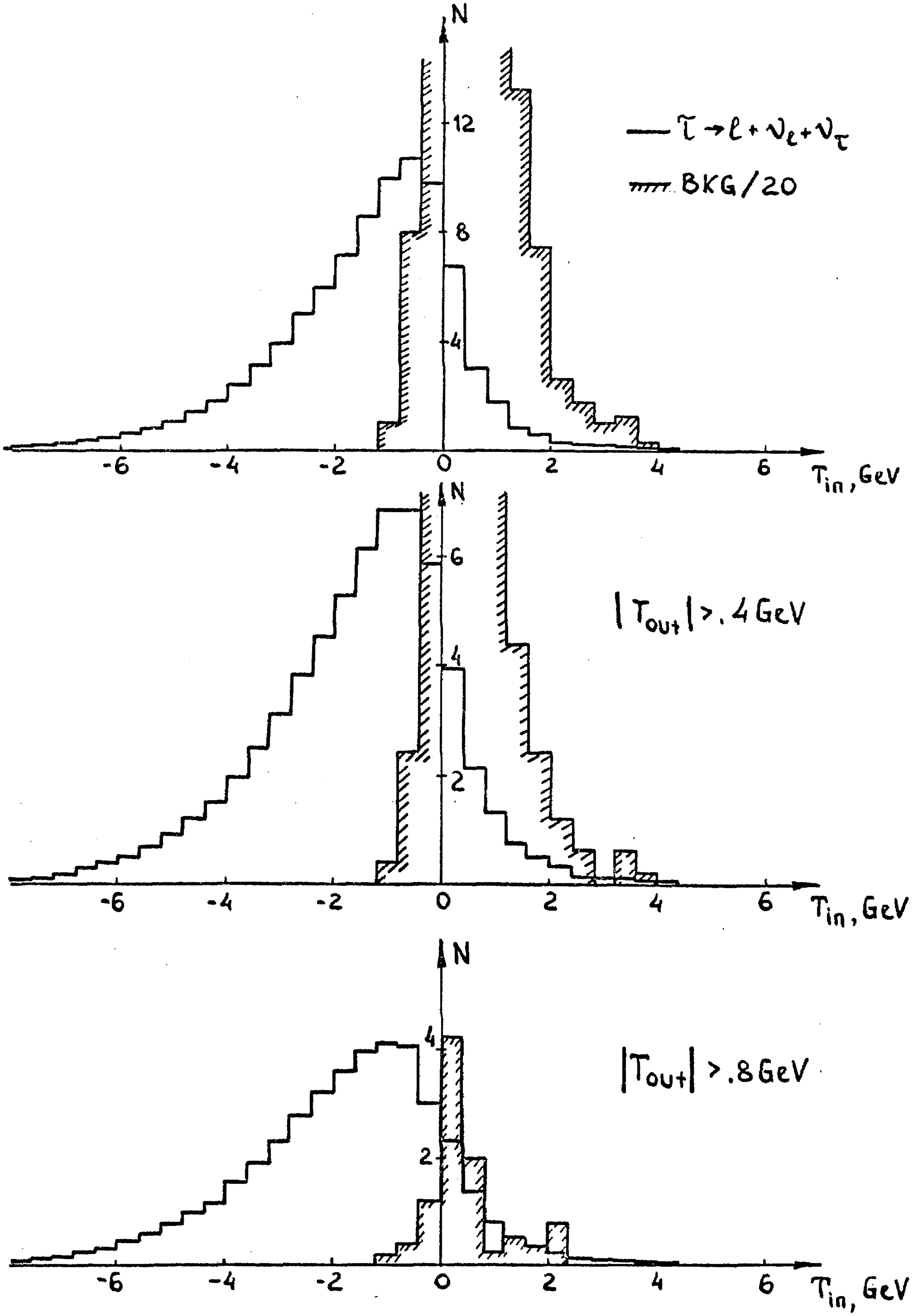

N
12
8
4
$\tau \to \ell + \nu_\ell + \nu_\tau$
BKG/20
-6
-4
-2
0
2
4
6
T_{in}, GeV
N
6
4
2
$|T_{out}| > .4$ GeV
-6
-4
-2
0
2
4
6
T_{in}, GeV
N
4
2
$|T_{out}| > .8$ GeV
-6
-4
-2
0
2
4
6
T_{in}, GeV

Fig.5

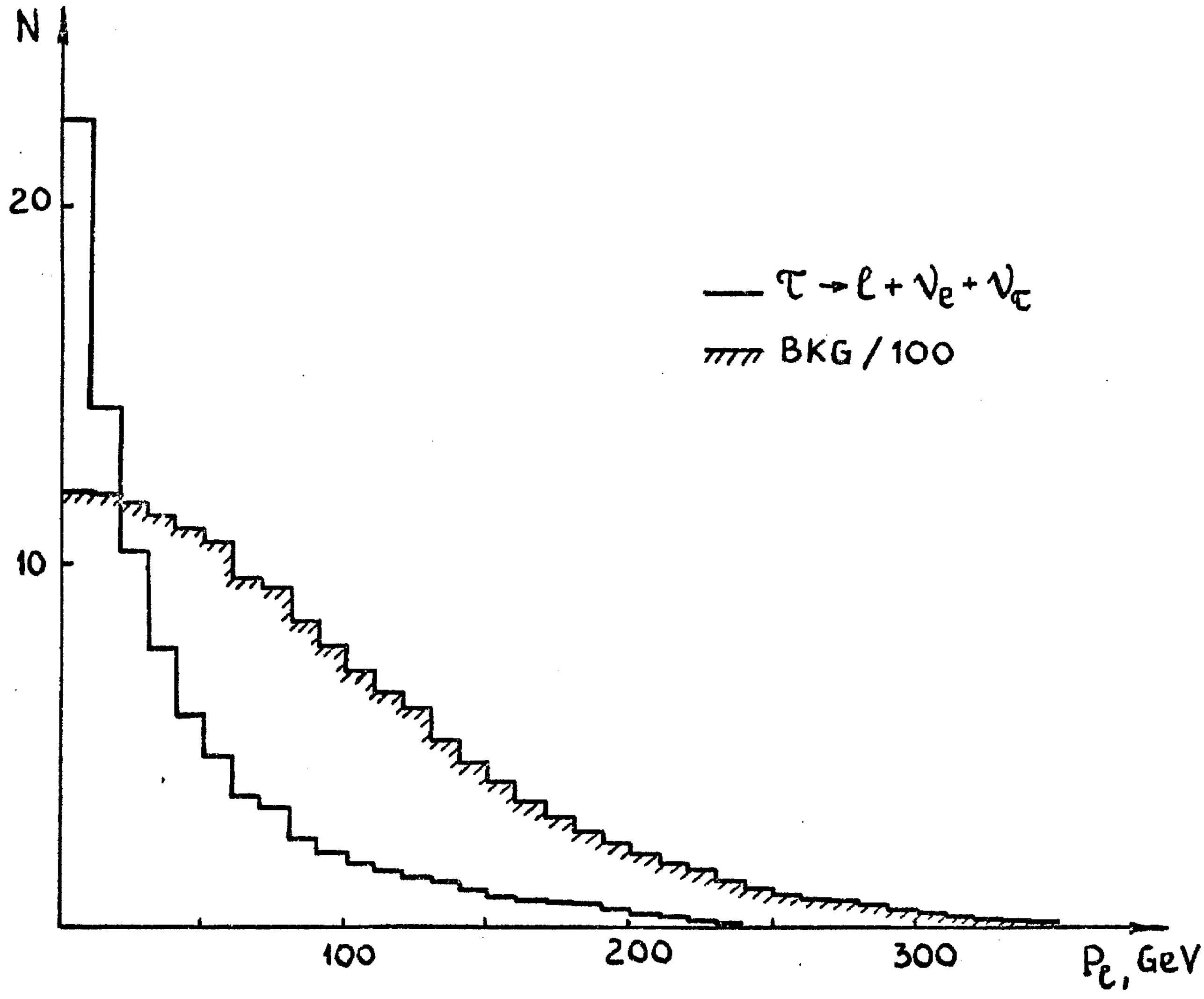

Fig. 6

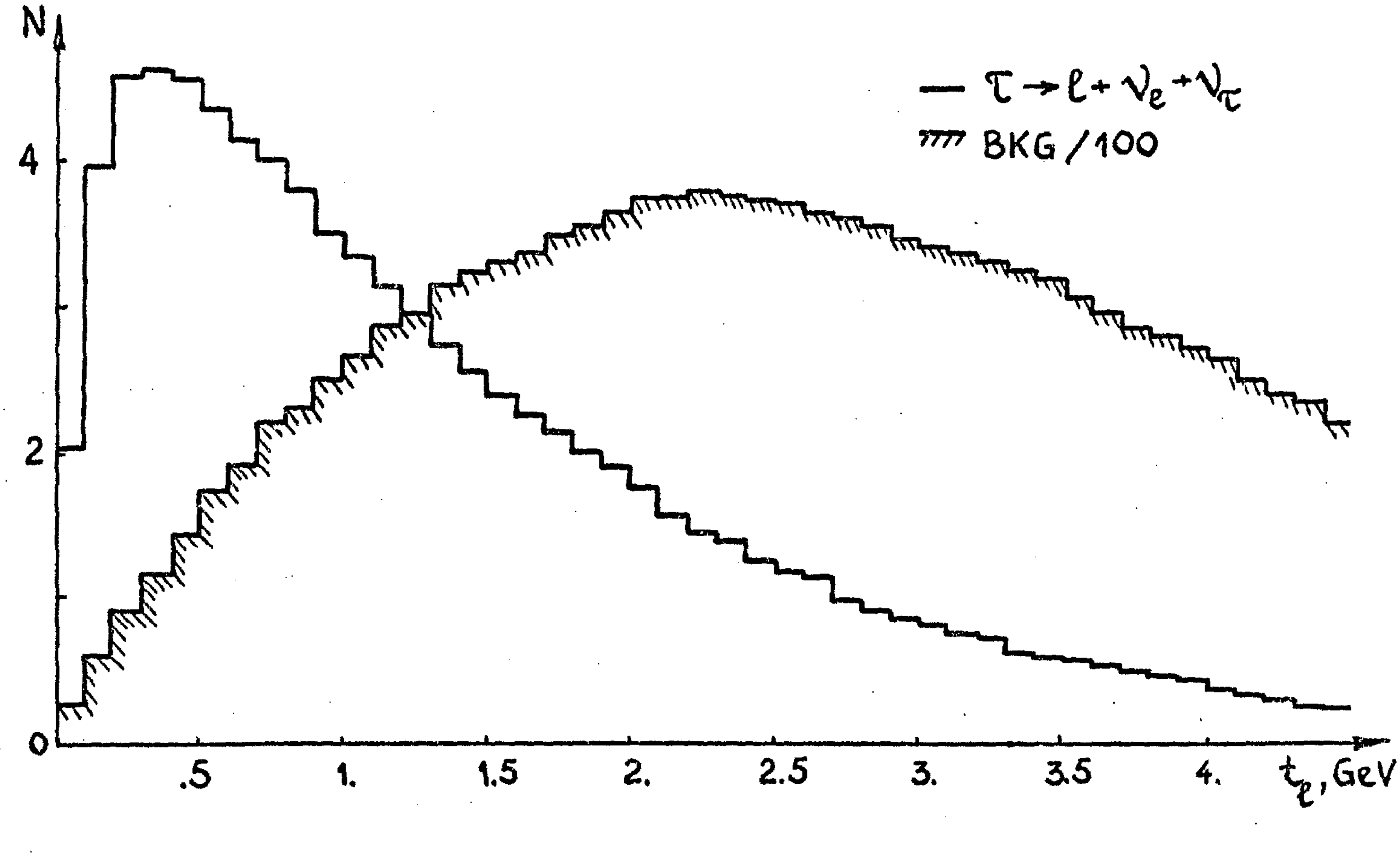

Fig. 7

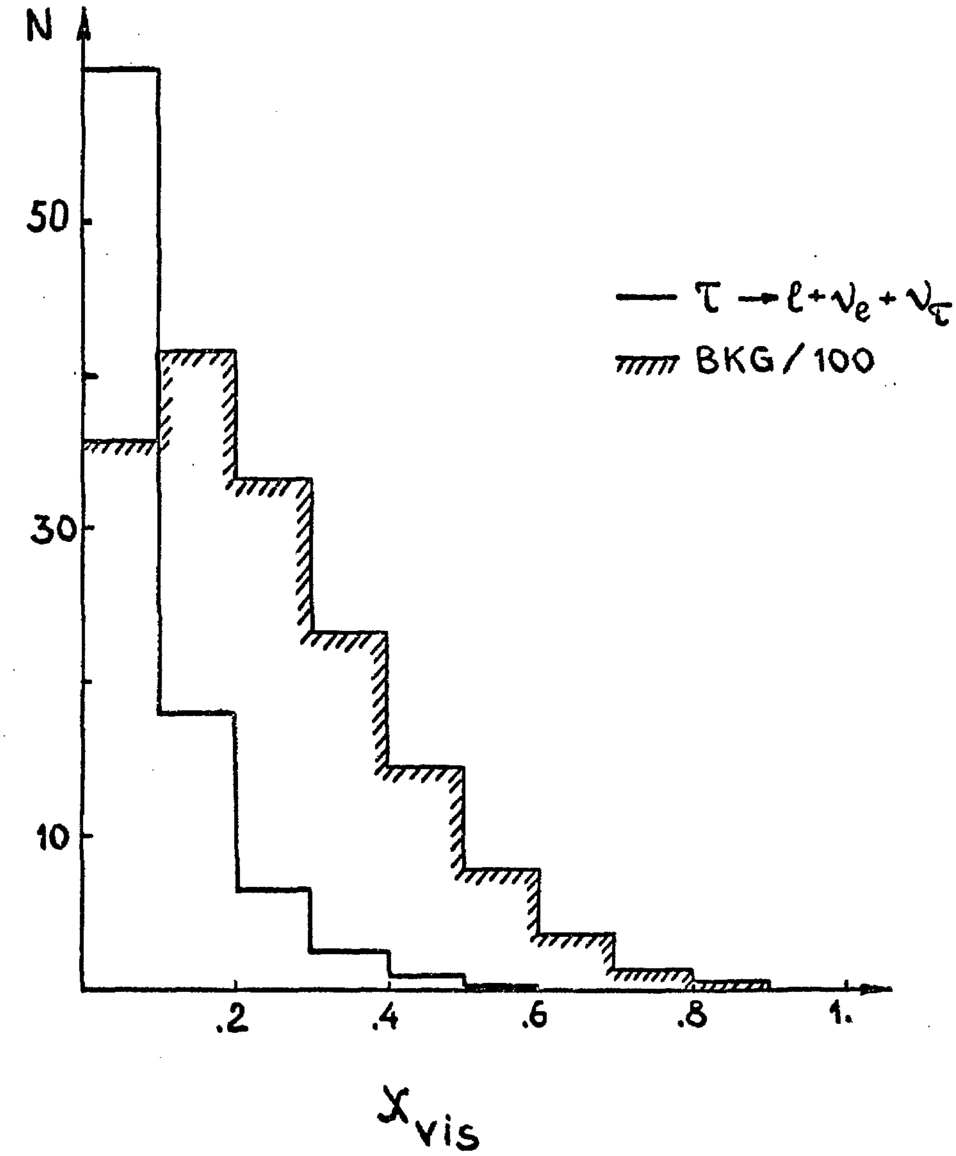

Fig. 8

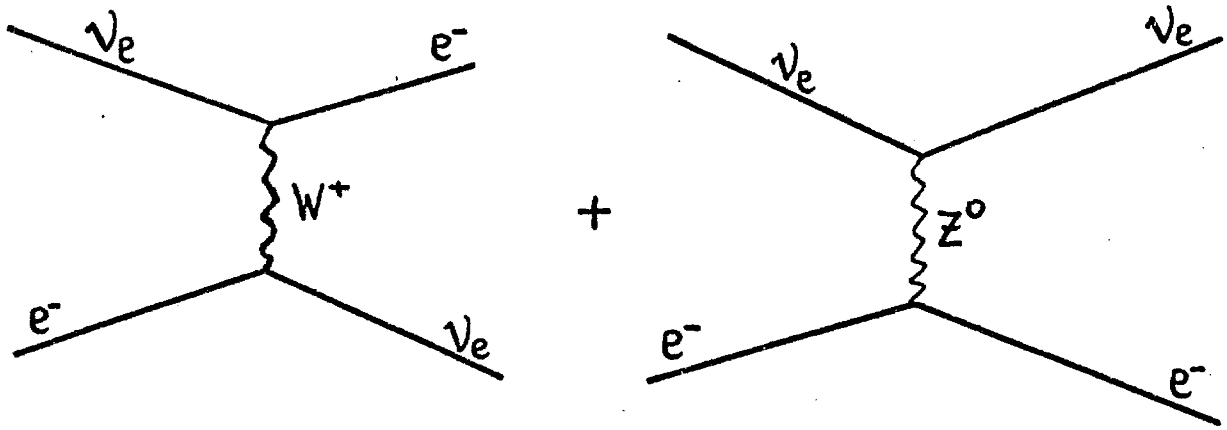

Fig. 9